Ocean circulation and biological processes drive seasonal variations of dissolved Al, Cd, Ni, Cu, and Zn on the Northeast Atlantic continental margin

Xue-Gang Chen [a,b,*,1], Dagmara Rusiecka [a,c,1], Martha Gledhill [a,c], Angela Milne [d], Amber L. Annett [c], Antony J. Birchill [d,e], Maeve C. Lohan [c], Simon Ussher [d], E. Malcolm S. Woodward [f], Eric P. Achterberg [a,c,*]

[a] GEOMAR Helmholtz Centre for Ocean Research Kiel, Kiel, Germany
[b] Ocean College, Zhejiang University, Zhoushan, China
[c] Ocean and Earth Sciences, National Oceanography Centre, University of Southampton, Southampton, UK
[d] School of Geography, Earth and Environmental Sciences, University of Plymouth, Plymouth, UK
[e] School of Environment, Geography and Geosciences, University of Portsmouth, UK.
[f] Plymouth Marine Laboratory, Plymouth, UK

ARTICLE INFO

ABSTRACT

Nutrients and nutrient-like dissolved trace metals (dTMs) are essential for the functioning of marine organisms and therefore form an important part of ocean biogeochemical cycles. Here, we report on the seasonal distributions of dissolved zinc (dZn), nickel (dNi), copper (dCu), cadmium (dCd), aluminum (dAl), and nutrients on the Northeast Atlantic continental margin (Celtic Sea), which is representative for temperate shelf seas globally. Variations in surface water dTM and nutrient concentrations were mainly regulated by seasonal changes in biological processes. The stoichiometry of dTMs (especially for dCu and dZn) and nutrients on the continental shelf was additionally affected by fluvial inputs. Nutrients and dTMs at depth on the continental slope were determined by water mass mixing driven by ocean circulation, without an important role for local remineralization processes. The Mediterranean Outflow Waters are especially important for delivering Mediterranean-sourced dTMs to the Northeast Atlantic Ocean and drive dTM:nutrient kinks at a depth of ~1000 m. These results highlight the importance of riverine inputs, seasonality of primary production and ocean circulation on the distributions of nutrients and nutrient-like dTMs in temperate continental margin seas. Future climate related changes in the forcing factors may impact the availability of nutrients and dTMs to marine organisms in highly productive continental shelf regions and consequently the regional carbon cycle.

1. Introduction

Dissolved (< 0.2 μm) bioactive trace metals (dTMs) including zinc (Zn), nickel (Ni), copper (Cu) and perhaps cadmium (Cd), are important micronutrients in the ocean. Zinc, Ni, and Cu are involved in enzymatic processes required for phytoplankton functioning (La Fontaine et al., 2002; Mahaffey et al., 2014; Twining and Baines, 2013) and Cd is taken up as a divalent metal and may substitute Zn in carbonic anhydrase (Horner et al., 2013). Low supply of dTMs could potentially affect marine ecosystem structure and function (Lohan and Tagliabue, 2018;

Morel and Price, 2003). Due to their biological uptake, the vertical distributions of dissolved Zn (dZn), Ni (dNi), Cu (dCu), and Cd (dCd) resemble those of nutrients (nitrate+nitrite [TN], phosphate [P], and silicic acid [Si]) (Bruland et al., 2014). These dTMs typically exhibit seasonally depleted concentrations in surface waters due to phytoplankton uptake (Moore et al., 2013; Morel and Price, 2003) and elevated levels at depth due to remineralization of sinking organic particles (Boyd et al., 2017). Nutrients and bioactive dTMs therefore show significant positive correlations with for example the dCd-P relationships in the global ocean (Boyle et al., 1976; Middag et al., 2018;

Wu and Roshan, 2015; Xie et al., 2015), and dZn-P, dNi-P and dCu-Si relationships in the South Atlantic (Wyatt et al., 2014) and Southern Oceans (e.g., Janssen et al., 2020; Saito et al., 2010).

The linear relationships between bioactive dTMs and nutrients usually show pronounced changes in slopes (kinks), e.g., in the case of P at concentration of ~1.3 μM for the Cd-P correlation (Cullen, 2006; de Baar et al., 1994). The origin of such kinks (especially the Cd:P kink) has been debated over the last decades. Some hypotheses point towards deeper regeneration of Cd relative to P (Boyle, 1988; Roshan and DeVries, 2021), or enhanced Cd uptake due to the limitation of bio-essential elements in surface waters (Cullen, 2006; Sunda and Huntsman, 2000). Kinks are also hypothesized to be associated with the chemical replacements between Co, Zn, and Cd in carbonic anhydrase in phytoplankton (Morel et al., 1994; Price and Morel, 1990) or a changing bioavailability of Cd through organic complexation (Bruland, 1992). Recent studies demonstrated that the mixing of water masses with different Cd:P ratios could be pivotal for the observed kinks (Baars et al., 2014; Middag et al., 2018; Xie et al., 2015). In addition, external sources of trace metals such as continental inputs and dust deposition can also affect bioactive dTM distributions in the ocean, and these inputs can be traced by dissolved aluminum (dAl) (Han et al., 2008; Measures and Edmond, 1988; Menzel Barraqueta et al., 2018). The ongoing debate on the drivers underpinning bioactive dTM distributions requires further investigations into co-occurrence of nutrients and bioactive dTMs and their relationships. Resolving this issue would improve our understanding of biogeochemical cycles in paleo – and modern oceans.

Continental margins with their shelves and slopes are gateways between terrestrial systems and open oceans. The disproportionately high primary production and particulate organic carbon export make continental margins important transition zones for the marine carbon cycle (Muller-Karger et al., 2005; Simpson and Sharples, 2012). Primary production in shelf seas, particularly in temperate shelf seas, results in a net drawdown of atmospheric CO_2. The shelf sea carbon pump subsequently transfers the captured carbon to the open ocean (Thomas et al., 2004). The Northeast (NE) Atlantic continental margin (Celtic Sea) is a typical temperate shelf sea and is representative for such systems globally because of its enhanced and seasonal primary productivity, seasonal co-limitation of phytoplankton growth by nitrate and Fe (Birchill et al., 2017), seasonal stratification, and occurrence of both fluvial and benthic inputs of redox sensitive TMs (including Fe and Mn) (Chen et al., 2023). Here, we report the seasonal distributions of dTMs (with focus on dCd, dCu, dNi, and dZn) and nutrients on the NE Atlantic continental margin, which is characterized by large seasonal variations in biological productivity (Birchill et al., 2017), complex bathymetry and dynamic water circulation (Fig. 1a). A high sampling resolution over three seasons (Fig. 1b) offers a unique opportunity to determine the influence of terrestrial inputs, biogeochemical processes, and ocean circulation on the seasonal variations of bio-essential dTMs and their relationships with nutrients.

2. Methods

2.1. Sampling

Samples were collected on cruises with *RRS Discovery* during three different seasons: an autumn cruise in November 2014 (DY018), a spring
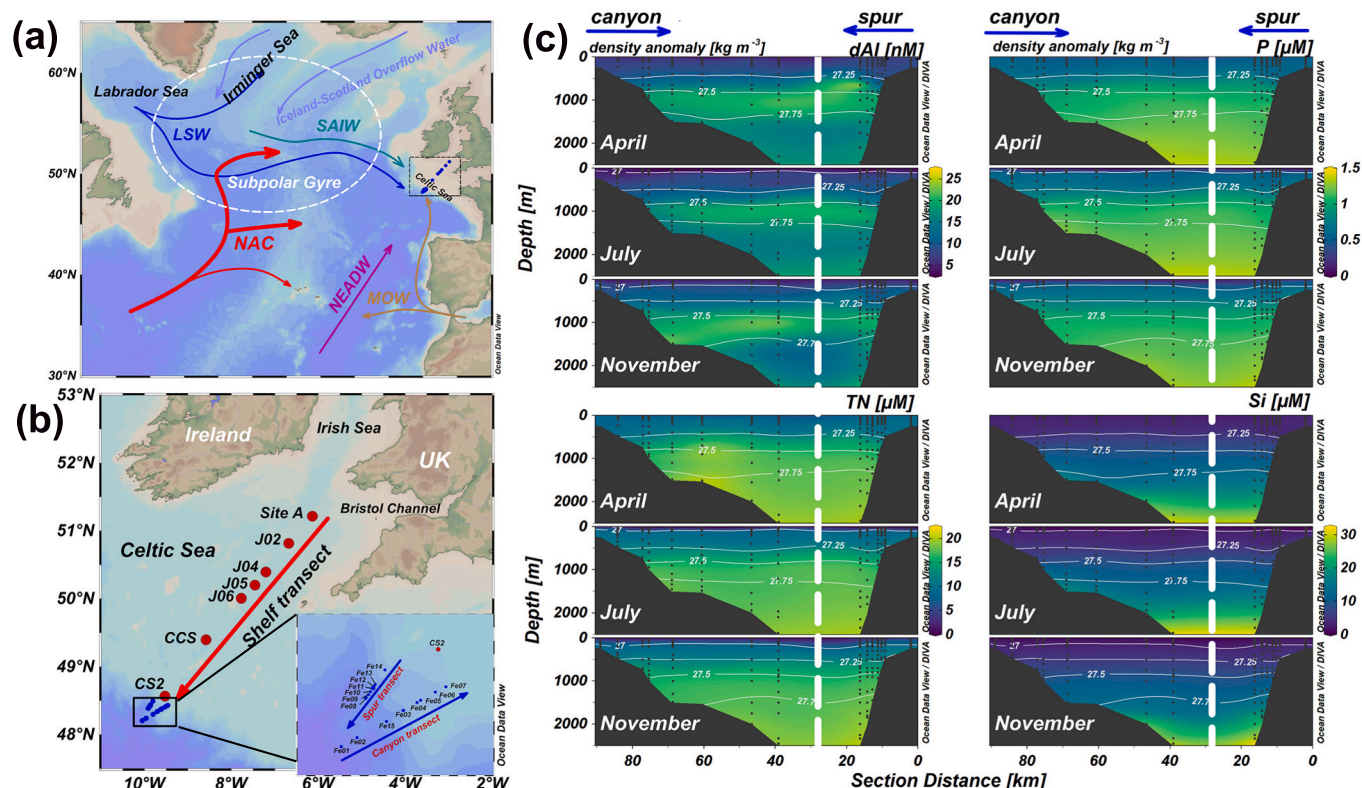
Fig. 1. (a) The schematic circulation of water masses (NAC: North Atlantic Current; LSW: Labrador Sea waters; SAIW: Sub-Arctic Intermediate Waters; MOW: Mediterranean Outflow Waters; NEADW: Northeast Atlantic Deep Waters) in the North Atlantic Ocean; (b) Sampling transects and locations on the Northeast Atlantic continental margin (Celtic Sea). The red and blue arrows define the shelf and slope sections, respectively, for Fig. 2 and Fig. 3. (c) Section plots of dissolved aluminum (dAl), phosphate (P), nitrate+nitrite (TN), and silicic acid (Si) along the slope transect during expeditions in November 2014 (DY018), April 2015 (DY029), and July 2015 (DY033) in Celtic Sea. The directions of the canyon and spur transects are indicated by blue arrows. The dashed black lines separate the canyon and spur transects. (For interpretation of the references to colour in this figure legend, the reader is referred to the web version of this article.)

cruise in April 2015 (DY029), and a summer cruise in July 2015 (DY033). Each season we conducted one transect on the continental shelf of the Celtic Sea from station Site A near the Bristol channel to station CS2 near the shelf break (Fig. 1b). Two off-shelf transects were conducted along a canyon (stations Fe01 - Fe07, Fe15) and a spur (stations Fe08 - Fe14) during each season.

Seawater samples for dTM analyses were collected following GEO-TRACES protocols (Cutter et al., 2017). Seawater samples were collected using 24 × 10 L Teflon coated trace metal clean Ocean Test Equipment (OTE) samplers positioned on a Titanium rosette frame. All OTE bottles were pressurized in a clean room with filtered (0.2 μm PTFE, Millex-FG 50, Millipore) compressed air. Seawater samples were filtered in-line using filter capsules (0.2 μm pore size; Sartorius, Sartobran P) into acid washed 125 mL low-density polyethylene bottles (Nalgene). All samples were acidified to pH of ~1.8 with ultra-pure hydrochloric acid (UpA Romil) in a laminar flow hood and stored double-bagged in ziplock bags.

2.2. Analyses

Trace metal samples were processed and analyzed at GEOMAR as outlined in Rapp et al. (2017). In detail, seawater samples were sub-sampled (15 mL) into fluorinated ethylene propylene bottles in a laminar flow hood. All sample bottles were spiked with 100 μL of diluted enriched isotope spike. Then, seawater samples were pre-concentrated by an automated system (SC-4 DX SeaFast pico; ESI) with online pH buffering and seawater matrix removal. Preconcentrated samples were analyzed by high-resolution inductively coupled plasma-mass spectrometry (HR-ICP-MS; Thermo Fisher Element XR) in low resolution (R = 300) for ^{110}Cd, ^{111}Cd, ^{115}In and in medium resolution (R = 4000) for ^{60}Ni, ^{62}Ni, ^{63}Cu, ^{65}Cu, ^{66}Zn, and ^{68}Zn. Reference materials, SAFe GEO-TRACES S and D1 were used to check the accuracy and precision of the measurements and the results were consistent with consensus values (Table 1).

Seawater samples for dAl were sub-sampled into acid washed 50 mL plastic tubes. An aluminum spectrofluorometric complex was obtained following the addition of lumogallion (Hydes and Liss, 1976) at pH 5.0–5.5 adjusted by addition of ammonium acetate buffer and the samples heated for 3 h at 55 °C. Samples were then analyzed by a spectrofluorometer (Cary Eclipse Fluorometer). The measured dAl concentrations of a reference standard (GS) were consistent with consensus values (Table 1).

Large volume samples for radium (Ra) analysis were collected from Niskin bottles deployed on a stainless-steel frame as per Birchill (2017). The samples for Ra were transferred into acid-washed 20 L collapsible

Table 1
GEOTRACES reference material results for dissolved Cd (dCd), Ni (dNi), Cu (dCu), Zn (dZn), and Al (dAl).

	dCd (pM)	dNi (nM)	dCu (nM)	dZn (nM)	dAl (nM)
Reported SAFe S		2.32 ± 0.22 (n = 10)	0.705 ± 0.130 (n = 8)	0.071 ± 0.025 (n = 8)	
Reported SAFe D1	979 ± 145 (n = 17)	8.41 ± 0.14 (n = 15)	2.19 ± 0.06 (n = 15)	7.13 ± 0.22 (n = 19)	
Consensus SAFe S		2.28 ± 0.09	0.52 ± 0.05	0.069 ± 0.010	
Consensus SAFe D1	991 ± 31	8.58 ± 0.26	2.27 ± 0.11	7.40 ± 0.35	
Reported GS					27.0 ± 0.6 (n = 6)
Consensus GS					27.5 ± 0.2

Consensus values obtained from https://www.geotraces.org/standards-and-reference-materials/.

containers, and slowly (<750 mL min^{-1}) passed through a column filled with 20 g of MnO$_2$-impregnated acrylic fiber to extract Ra from seawater (Moore, 2008). Fibers were rinsed with ultra-high purity water, and partially air dried to optimize emanation of the radon daughter (Sun and Torgersen, 1998). Then, the samples were counted immediately using a Ra Delayed Coincidence Counter [RaDeCC] (Moore, 2008; Moore and Arnold, 1996). Counting was repeated after ~30 (~90) days to determine the ^{224}Ra (^{223}Ra) activity supported by the parent isotopes ^{228}Th (^{227}Ac). Uncertainty calculations followed the methods of Garcia-Solsona et al. (2008). The efficiencies of the RaDeCC systems were calibrated and monitored using standards prepared from ^{227}Ac and ^{232}Th (Annett et al., 2013). Radium activities (^{224}Ra$_{xs}$ and ^{223}Ra$_{xs}$) are reported in excess of activity supported by the parent isotopes in the water column.

Unfiltered seawater samples for nutrients (TN, P, Si) were taken from the same OTE bottles as trace metal samples. They were sampled into 'aged' 10% HCl acid washed and de-ionized water rinsed high-density polyethylene bottles. Seawater sampling and handling for nutrient analysis was carried out where possible according to the GO-SHIP nutrient manual recommendations (Becker et al., 2020). Nutrient analysis was carried out on board within a few hours of sampling using a SEAL Quaatro segmented flow nutrient autoanalyzer using colorimetric analytical techniques described in Woodward and Rees (2001).

Turbidity was measured by an Aquatracka MKIII fluorometer (Chelsea Technologies Group) at a wavelength of 400 nm and a bandwidth of 80 nm. Conductivity, temperature, and depth (CTD) data were collected using a Seabird 911+ CTD system, and processed on board. Conductivity was measured by a Sea-Bird SBE 4C sensor and calibrated on-board using discretely collected salinity samples analyzed with a Guildline Autosal salinometer. Temperature was measured with Sea-Bird SBE 3plus (SBE 3P) temperature sensor. Dissolved oxygen was measured by a Sea-Bird SBE 43 oxygen sensor and calibrated against photometric on-board Winkler titration results. Apparent oxygen utilization (AOU) is calculated from the presumed oxygen concentrations under atmospheric saturation for a given temperature (θ) and salinity (S), subtracted from the observed dissolved oxygen concentrations.

$$AOU = \left[O_{2,sat}(\theta, S) \right] - [O_2]$$

2.3. Statistics and plots

Figs. 1, 2, 3, and 6 were created with Ocean Data View (5.6.2) software (Schlitzer, 2021) using DIVA gridding. All other plots and associated statistics were performed by *R* programming 4.2.0 with packages *tidyverse* (Wickham et al., 2019), psych (Revelle, 2017), and *ggpmisc* (Aphalo, 2022).

3. Results and discussion

Dissolved Cd, Zn, Ni, and Cu exhibited nutrient-like vertical distributions during all seasons on the NE Atlantic continental margin (Fig. 1c, Fig. 2, Fig. 3), with lowest concentrations in surface waters due to biological utilization, and elevated concentrations at depth ascribed to remineralization (Bruland et al., 2014; Moore et al., 2013). The canyon and spur transects showed comparable vertical profiles for dTMs and nutrients for each season and were combined as a slope transect (Fig. 1c, Fig. 2). In contrast to the relatively constant of bioactive dTM and nutrient concentrations at depth on the continental slope, the surface bioactive dTM and nutrient levels in the Celtic Sea showed pronounced seasonal variations (Table S1). Kinks in dTM:nutrient (e.g., dZn:P and dCu:P) ratios were observed on the continental slope at a depth of ~100 m and ~ 1000 m (Fig. 4). The shelf transect (Fig. 3) showed higher dCu, dNi, dZn, and Si concentrations than the slope transect (Fig. 1c, Fig. 2), accompanied by varying dTM: nutrient correlations.
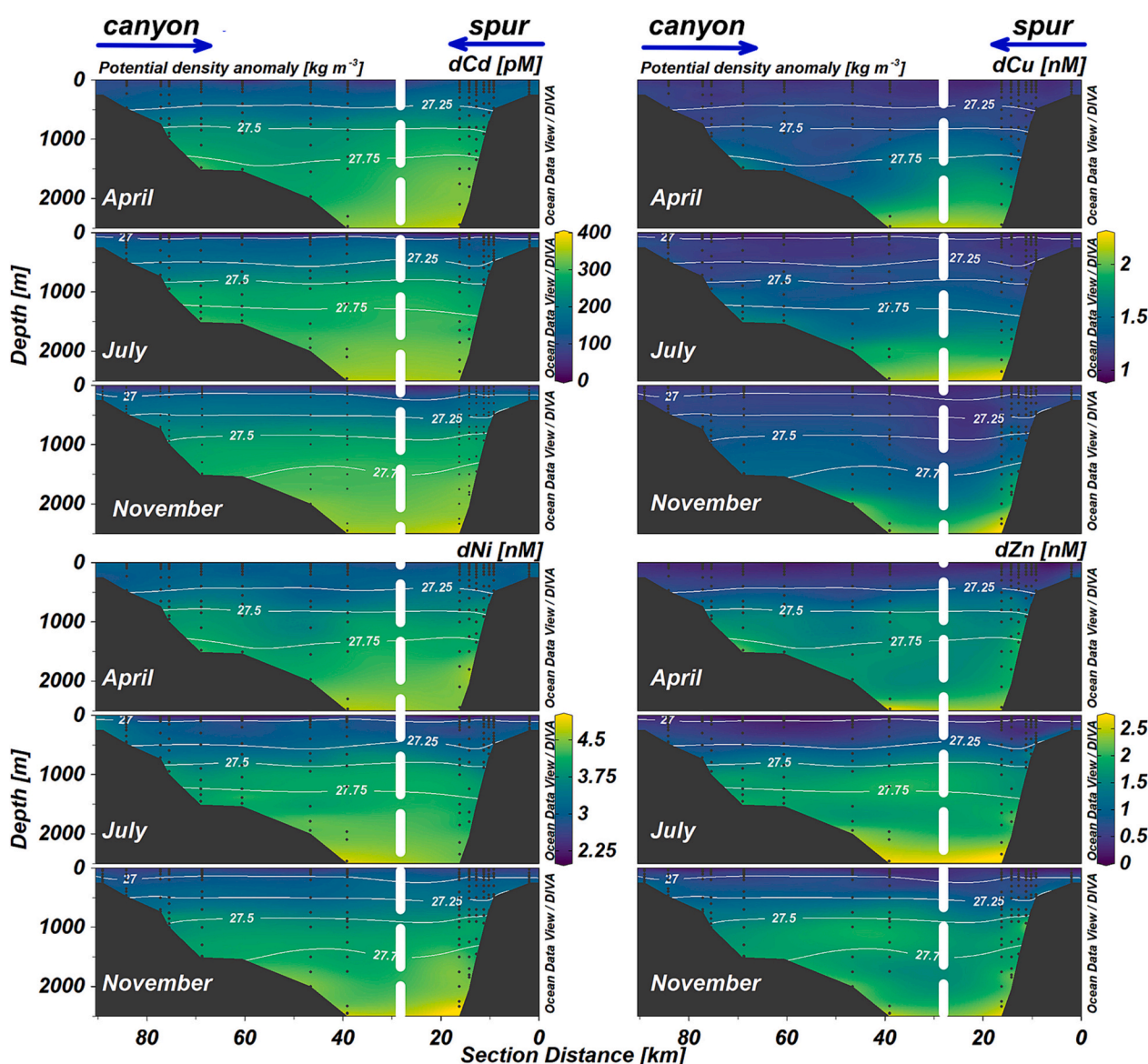
Fig. 2. Section plots of dissolved cadmium (dCd), copper (dCu), nickel (dNi), and zinc (dZn) on the slope of the Northeast Atlantic continental margin. Samples were taken in November 2014, April 2015, and July 2015, respectively. The section is defined in Fig. 1b. The directions of the canyon and spur transects are indicated by blue arrows. The dashed black lines separate the canyon and spur transects. (For interpretation of the references to colour in this figure legend, the reader is referred to the web version of this article.)

3.1. Biological influence on seasonal variations in surface dTM along the continental slope

A seasonal mixed layer (SML) with a depth of ∼ < 100 m occurred between spring and autumn on the continental slope (Supporting information: Hydrography). A decrease in dTM and nutrient concentrations in the SML (especially at depths <30 m) was observed between April 2015 and July 2015, due to biological utilization and water column stratification (Birchill et al., 2017) (Table S1). Enhanced phytoplankton activity was indicated by maxima in chlorophyll *a* levels in the SML in April 2015, and just beneath the SML in July 2015 (Birchill, 2017). Using the differences between the mean dTM values observed during the April and July cruises, the total drawdown of surface (depth < 30 m) dTMs and nutrients on the slope from spring to summer was: dCd 79.5 ± 45.1 pM, dCu 0.08 ± 0.11 nM, dNi, 0.67 ± 0.31 nM, dZn 0.10 ± 0.25 nM, P 0.35 ± 0.11 μM, TN 6.71 ± 1.83 μM, and Si 2.44 ± 0.47 μM (Table S1). The removal of dCd, dNi, P, and TN over this period was higher, and the drawdown of Cu was lower than reported for this

region for the period between January 1994 and June 1995 (TN 3.9 ± 3.9 μM, P 0.46 ± 0.51 μM, Si 2.2 ± 3.7 μM, Cd 39 ± 61 pM, Cu 0.34 ± 0.58 nM, Ni 0.5 ± 1.1 nM) (Cotté-Krief et al., 2002), and between March and June 1987 (Cd 30 ± 12 pM) (Kremling and Pohl, 1989). The decrease in dTM and nutrient concentrations was the consequence of phytoplankton uptake in spring and summer, and the overall "uptake" ratio of phytoplankton normalized to average P was:

$$(N_{19\pm5}Si_{7\pm1.3}P_1)_{1000}Ni_{1.9\pm0.9}Zn_{0.29\pm0.71}Cu_{0.23\pm0.31}Cd_{0.23\pm0.13}$$

The surface dTM and nutrient concentrations on the slope increased from July to November, and we assume this was due to internal cycling and not to significant changes in external supply. This phenomenon was accompanied by correlations comparable to the spring-summer period between dTMs/nutrients and AOU at AOU > 0 (Fig. S2). Therefore, the surface dTM and nutrient variations from summer to autumn was affected by the remineralization of organic particles. On the other hand, the increase in surface dTM and nutrient concentrations from November to April was attributed to resupply from subsurface waters (Birchill
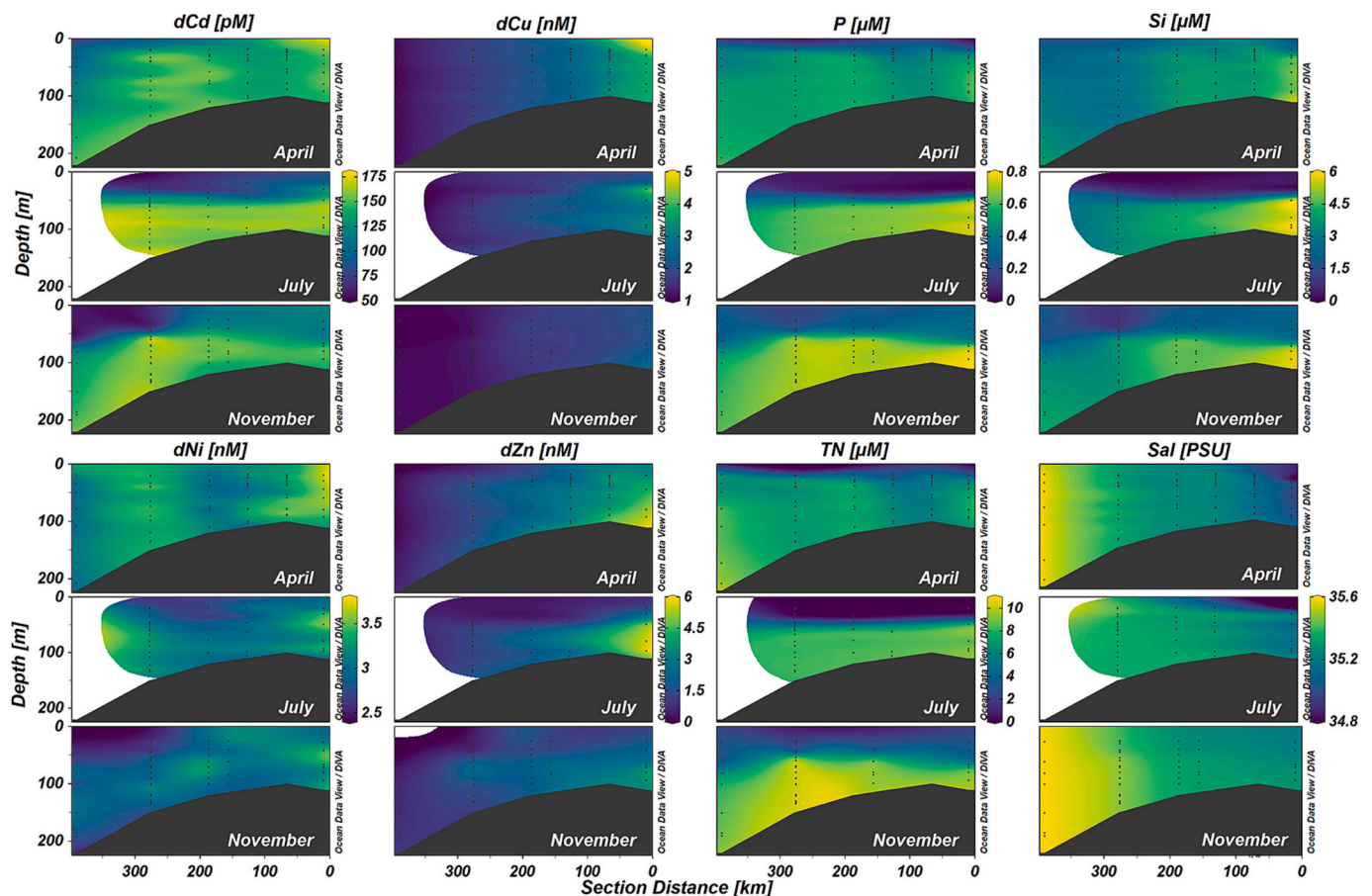
Fig. 3. Section plots of dissolved trace metals (dCd, dCu, dNi, dZn), salinity, and nutrients (nitrate+nitrite (TN), phosphate (P), silicic acid (Si)) on the continental shelf of the Northeast Atlantic Ocean. The section is defined in Fig. 1b. Samples were taken in November 2014, April 2015, and July 2015, respectively.

et al., 2017). Using concentration differences between July and November (Table S1), we estimated the apparent "remineralization" ratio of dTMs and nutrients normalized to P as:

$$(N_{15\pm13}Si_{6.8\pm3.4}P_1)_{1000}Ni_{1.9\pm2.2}Zn_{0.57\pm1.29}Cu_{0.43\pm0.71}Cd_{0.28\pm0.12}$$

and the "winter mixing" ratio estimated from the concentration differences between November and April observations as:

$$(N_{21\pm9}Si_{7.1\pm2.6}P_1)_{1000}Ni_{1.9\pm1.0}Zn_{0.10\pm1.19}Cu_{0.10\pm0.33}Cd_{0.19\pm0.20}$$

The estimated Zn:P and Cu:P ratios between "uptake" and "remineralization" varied by as much as a factor of 2, but the "winter mixing" ratios were as much as an order of magnitude lower, probably due to relatively limited seasonal variations and large concentration ranges observed for both metals (Table S1). The N:P, Si:P, Ni:P, and Cd:P ratios were relatively constant, indicating a close association of Ni and Cd with biological processes in surface waters across all seasons. The observed "uptake", "remineralization", and "winter mixing" ratios are close to the overall dTM:P ratios in the SML (depth of $< \sim 100$ m) ($P_{1000}Ni_{1.53\pm0.08}Zn_{0.37\pm0.07}Cu_{0.20\pm0.03}Cd_{0.21\pm0.01}$) (Table S2). The dTM:P ratio here is broadly consistent with the extended Redfield ratio of phytoplankton cultures ($(N_{16}P_1)_{1000}Zn_{0.80}Cu_{0.38}Cd_{0.21}$) (Ho et al., 2003). Therefore, the positive correlations between dTMs and nutrients in the SML on the continental slope across all seasons (Fig. 4) generally reflected the seasonal cycling of biological uptake in spring and summer, remineralization of organic particles in autumn, followed by winter mixing.

3.2. Additional fluvial inputs of dTMs on the shelf

Seasonality of biological processes also affected the dTM and

nutrient distributions on the shelf of the NE Atlantic Ocean. Using station CCS (central Celtic Sea) as an example (Fig. 5), surface dTM and nutrient concentrations decreased from April to July due to phytoplankton uptake. Subsurface (depths >50 m) nutrient and dCd levels increased from April to November due to remineralization of sinking organic particles (Birchill et al., 2017; Lohan and Tagliabue, 2018). In contrast, subsurface dCu and dNi gradually decreased from spring to autumn, possibly reflecting the impact of removal mechanisms and/or water mass mixing. The overall dTM:P ratios on the shelf varied greatly between sampling locations (Fig. S3). For instance, the slopes of dZn-P relationship decreased from 3.58×10^{-3} at site A to 2.16×10^{-3} at station CS2. These variations were accompanied by decreasing dTM concentrations with distance offshore, suggesting the dTM stocks on the shelf were additionally supplied by external sources. Benthic sediments were likely not an important source for the enhanced dTMs, since dTM concentrations did not change significantly with $^{223}Ra_{xs}$ and $^{224}Ra_{xs}$ activities (Fig. S4). Atmospheric deposition also likely played a minor role in the increase in dTM concentrations closer to shore, because dAl, a tracer of atmospheric dust inputs (Johnson et al., 2010; Menzel Barraqueta et al., 2019), did not indicate surface enrichments (Fig. 1c).

Instead, an increasing salinity with distance offshore (Fig. 3) and strong negative correlations between dTMs and salinity suggest dTM (especially for dCu and dZn) concentrations (Fig. S5) were augmented by a dTM-rich low-salinity endmember, e.g., riverine input from the British Isles through the Irish Sea and/or the Bristol channel (Achterberg et al., 1999; Kremling and Hydes, 1988). Based on the correlations between subsurface (depth of 50–200 m to exclude surface biological activity) dTMs, nutrients, and salinity in April when significant correlations were observed, the low-salinity endmember at a salinity of
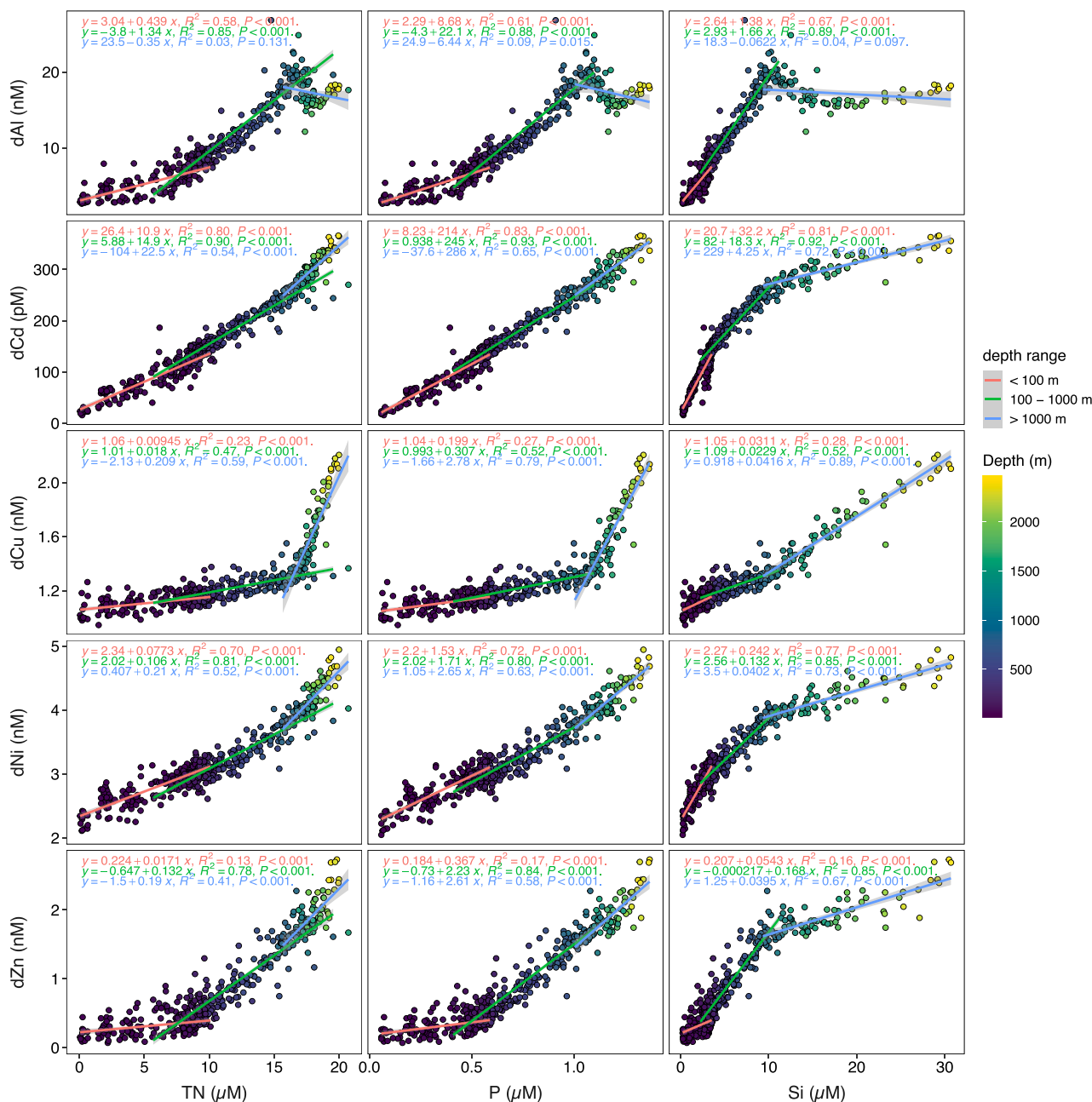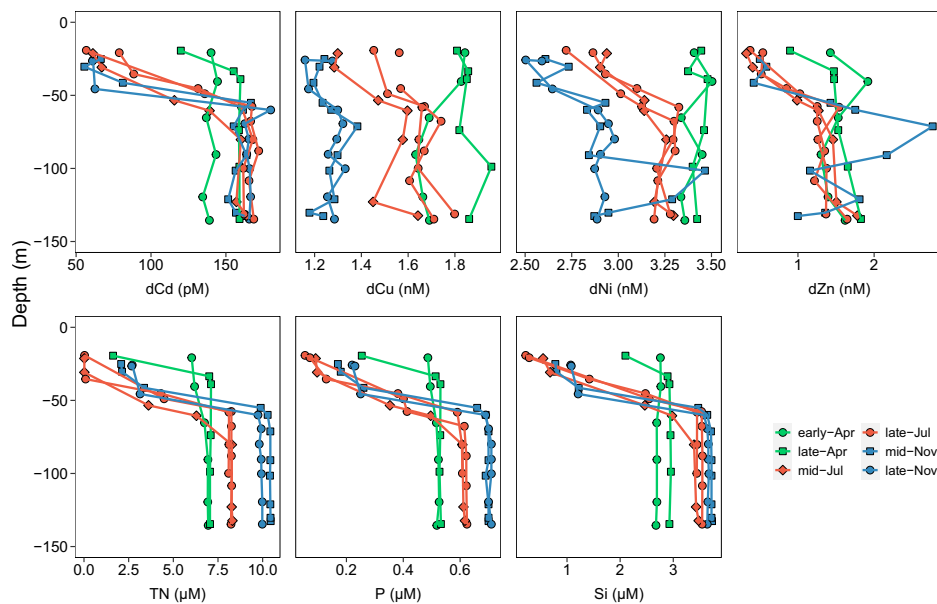
Fig. 4. Correlations between dissolved trace metals (dAl, dCd, dCu, dNi, dZn) and nutrients (nitrate+nitrite (TN), phosphate (P), silicic acid (Si)) on the continental slope of Celtic Sea. Linear regression models are applied to surface (< 100 m), 100–1000 m (density generally 27.25–27.62 kg m^{-3}), and > 1000 m (density > 27.62 kg m^{-3}), respectively.

33.5 (typical salinity of the Irish Sea and Bristol Channel) were calculated as: dCd, 144 $\pm$ 59 pM; dCu, 13.0 $\pm$ 1.2 nM; dNi, 4.45 $\pm$ 1.11 nM; dZn, 22.2 $\pm$ 3.2 nM; TN, 9.45 $\pm$ 3.85 μM; P, 0.80 $\pm$ 0.23 μM; and Si, 12.9 $\pm$ 1.8 μM. The calculated dCd and dNi endmember concentrations are comparable with observed dTM concentrations (dCd, 0.22 nM; dNi, 5.2 nM) in the low-salinity waters around the British Isles (Kremling and Hydes, 1988), suggesting a relatively conservative behavior of fluvially supplied dCd and dNi. The endmember dCu concentration is twice as high as reported values (6.7 nM) (Kremling and Hydes, 1988), possibly reflecting additional dCu from the Bristol Channel or temporal variations in riverine dCu concentrations. The enrichment of dCu and dZn relative to P in the low-salinity endmember produced gradually decreasing dCu:P and dZn:P ratios with increasing distance stretching from Site A to CS2 (Fig. S3). Fluvial inputs were not a major source of dCd and dNi, resulting in increasing dCd:P and dNi:P ratios with

offshore distance.

The low-salinity endmember showed strong seasonal variations in dCu and dZn concentrations (Fig. S5). The highest endmember dCu and dZn concentrations were observed in July 2015, with 17.4 $\pm$ 1.9 nM and 43.3 $\pm$ 4.2 nM, respectively. Data from the November 2014 cruise showed the lowest dCu (9.04 $\pm$ 1.26 nM) and dZn (14.7 $\pm$ 6.2 nM) concentrations for the low-salinity endmember. These variations probably reflect seasonal changes in fluvial dCu and dZn concentrations. Fluvial inputs at a given salinity generally show elevated dTM concentrations in summer relative to other seasons, due to enhanced sediment re-suspension and/or benthic sedimentary input via reductive dissolution of TM carrying Mn and Fe oxyhydroxide phases in the source regions (Hu et al., 2022; Mora et al., 2009; Waeles et al., 2005). Furthermore, the seasonal variations in the low-salinity endmember can be influenced by remineralization at stations away from the fluvial

Fig. 5. Seasonal variations of dissolved trace metal (dTMs: dCd, dCu, dNi, dZn) and nutrient (nitrate+nitrite [TN], phosphate [P], silicic acid [Si]) concentrations of water columns at station CCS (central Celtic Sea). Note that some *x* ranges are not starting from 0.

source, as indicated by the elevated subsurface dTM and nutrient levels at station CCS relative to other stations in autumn. Therefore, the distributions of dTMs and nutrients as well as their correlations on the continental shelf were balanced by riverine inputs and the seasonality of biogeochemical processes.

3.3. Water mass mixing drive metal:P kinks at depth

The waters on the NE Atlantic continental slope at depths between the SML and potential density of 27.62 kg m^{-3} (depth ~ 1000 m) are characterized by the presence of East North Atlantic Central Waters (ENACW), Mediterranean Outflow Waters (MOW), and Sub-Arctic Intermediate Waters (SAIW) (Rusiecka et al., 2018) (Fig. S6). An increasing MOW contribution with depth is accompanied by increasing dTM and nutrient concentrations. Waters with potential density > 27.62 kg m^{-3} are characterized by a gradually decreasing MOW contribution, and increasing contributions of Labrador Sea Water (LSW) and North East Atlantic Deep Waters (NEADW) (Fig. S6). The dTM and nutrient concentrations continuously increased with depth, showing dCd of ~350 pM, dCu of ~2.2 nM, dNi of ~5 nM, dZn of ~2.7 nM in bottom waters (Table S1). These concentrations are similar to reported deep dCd (310 ± 26 pM), dNi (4.1 ± 0.4 nM), and dCu (1.56 ± 0.33 nM) values for this region (Cotté-Krief et al., 2002) and consistent with reported deep water dTM and nutrient values in the North Atlantic Ocean (Achterberg et al., 2021; Saager et al., 1997).

No apparent kinks were identified for dCd:P (260 ± 3 μmol mol^{-1}), dNi:P (1.94 ± 0.04 mmol mol^{-1}), and dZn:P (2.26 ± 0.04 mmol mol^{-1}) in waters >100 m (Table S2). These ratios here are similar to those reported for the North Atlantic Ocean with dCd:P of 278 ± 3 μmol mol^{-1}, dNi:P of 2.01 ± 0.08 mmol mol^{-1}, and dZn:P of 1.77 ± 0.16 mmol mol^{-1} at P concentrations between 0.5 and 1.5 μM (GEOTRACES Intermediate Data Product Group, 2021; Middag et al., 2018; Roshan and Wu, 2015). The absence of dCd:P kinks agrees with the linear dCd – P relationship for *P* < 1.3 μmol kg^{-1} (Cullen, 2006; de Baar et al., 1994; Frew and Hunter, 1992; Middag et al., 2018). In contrast, the dCu:P ratio on the slope of the NE Atlantic continental margin increased from 0.31 mmol mol^{-1} at 100–1000 m to 2.78 mmol mol^{-1} at depths >1000 m and the dAl concentrations showed pronounced zigzag-shaped variations with increasing P levels (Fig. 4). Considering the small variations in surface dCu concentrations and that Al is not a bio-essential element,

changes in subsurface dCu:P and dAl:P ratios with water depth should reflect physical (e.g., water mass mixing) rather than biological processes.

We estimated the elemental composition of each water mass using a three-step calculation (Table 2). (1) At potential density < 27.62 kg m^{-3} (depths < ~ 1000 m), endmember MOW concentrations were calculated from the positive linear correlations with dTM concentrations (Fig. S7). (2) Nutrients and dTMs contributed by MOW were removed. At potential density > 27.62 kg m^{-3}, the residual dTMs were contributed by LSW, NEADW, and SAIW, where the endmember SAIW concentrations were calculated from the significant negative linear relationship between the corrected SAIW contribution and corrected dTM concentrations (Fig. S8). The endmember NEADW concentrations were evaluated at LSW < 1% (Fig. S9a). (3) Finally, the endmember concentrations of LSW and ENACW were estimated by removing the contributions of the MOW, SAIW, and NEADW (Fig. S9b and c).

All dTMs and nutrients showed significant correlations with percentage contributions of LSW and ENACW at the final step, despite uncertainties propagating during each step in the calculations. The predicted dTM concentrations, reconstructed by direct multiplication of water mass fractions with their endmember values, illustrate almost identical values with the observed concentrations with very low residuals (Fig. 6). For instance, residuals of dCu, dNi, and dZn are mostly <0.1 nM and the dCd residuals mostly range from −10 to 10 pM. Furthermore, the residuals are within the measurement uncertainties of the raw data used for the OMP analysis, suggesting that the residuals may be determined by TM measurements rather than the OMP analysis. The calculated endmember concentrations of NEADW agree with deep water (> 4000 m) concentrations in the NE Atlantic Ocean (GEOTRACES Intermediate Data Product Group, 2021; Liu and Tanhua, 2021), where NEADW is a persistent feature (García-Ibáñez et al., 2018, 2015; Reinthaler et al., 2013; van Aken, 2000a). The predicted dTM concentrations of MOW are also consistent with previous observations. Specifically, the differences in dCu, dNi, and dZn between our calculations and previous observations are generally <10% in relative standard deviations (RSD). Therefore, these dTMs have behaved in a relatively conservative manner during ocean circulation and water mass mixing. Dissolved Al and Cd showed larger differences (RSD > 20%) between our calculated endmember and observed concentrations. Our calculated dCd endmember is higher than observed concentrations, probably due

Table 2

Estimated endmember concentrations (with 95% confidence levels) of water masses on the Northeast (NE) Atlantic Ocean. ENACW: East North Atlantic Central Waters, SAIW: Sub-Arctic Intermediate Waters, MOW: Mediterranean Outflow Waters, LSW: Labrador Sea Water, NEADW: North East Atlantic Deep Waters.

| Water mass	dAl (nM)	dCd (pM)	dCu (nM)	dNi (nM)	dZn (nM)	P* (μM)	TN* (μM)	Si* (μM)
ENACW	5.91 ± 1.13	111 ± 9	1.15 ± 0.05	2.64 ± 0.12	0.31 ± 0.13	0.10	0.1	0.85
SAIW	5.17 ± 1.04	134 ± 16	1.12 ± 0.08	2.96 ± 0.13	0.28 ± 0.15	0.86	13.0	6.3
MOW	29.6 ± 1.0	366 ± 9	1.47 ± 0.04	4.61 ± 0.11	2.71 ± 0.12	1.20	17.5	9.0
MOW[1]	35.6 ± 6.8	202 ± 45	1.21 ± 0.07	–	1.99 ± 0.24			
MOW[2]		~ 160		~ 4	~ 2			
MOW[3]	20.1 ± 1.5	264 ± 11	1.32 ± 0.03	3.90 ± 0.11	1.68 ± 0.14			
LSW	16.9 ± 4.2	262 ± 56	1.94 ± 0.44	4.50 ± 0.55	1.65 ± 0.65	1.05	16.5	10.0
NEADW	15.9 ± 4.9	475 ± 53	2.20 ± 0.27	5.28 ± 0.46	3.02 ± 0.54	1.65	22.5	45.0
NEADW[4]	23.1 ± 2.3	372 ± 14	2.75 ± 0.12	5.40 ± 0.05	3.02 ± 0.29			

* Pre-determined nutrient concentrations, adopted from García-Ibáñez et al. (2015) and GLODAP v2 (Olsen et al., 2019) following Rusiecka et al. (2018).

[1] Calculated from the water columns with depths of 900–1400 m near the Gibraltar channel where the occurrence of MOW is significant (Middag et al., 2022; Rolison et al., 2015). Data obtained from (GEOTRACES Intermediate Data Product Group, 2021).

[2] From Middag et al. (2022).

[3] Average values of water columns with depths of 950–1050 m on the NE Atlantic continental slope (this study).

[4] Calculated from water columns with depths of >4000 m on the NE Atlantic Ocean. Data obtained from (GEOTRACES Intermediate Data Product Group, 2021).
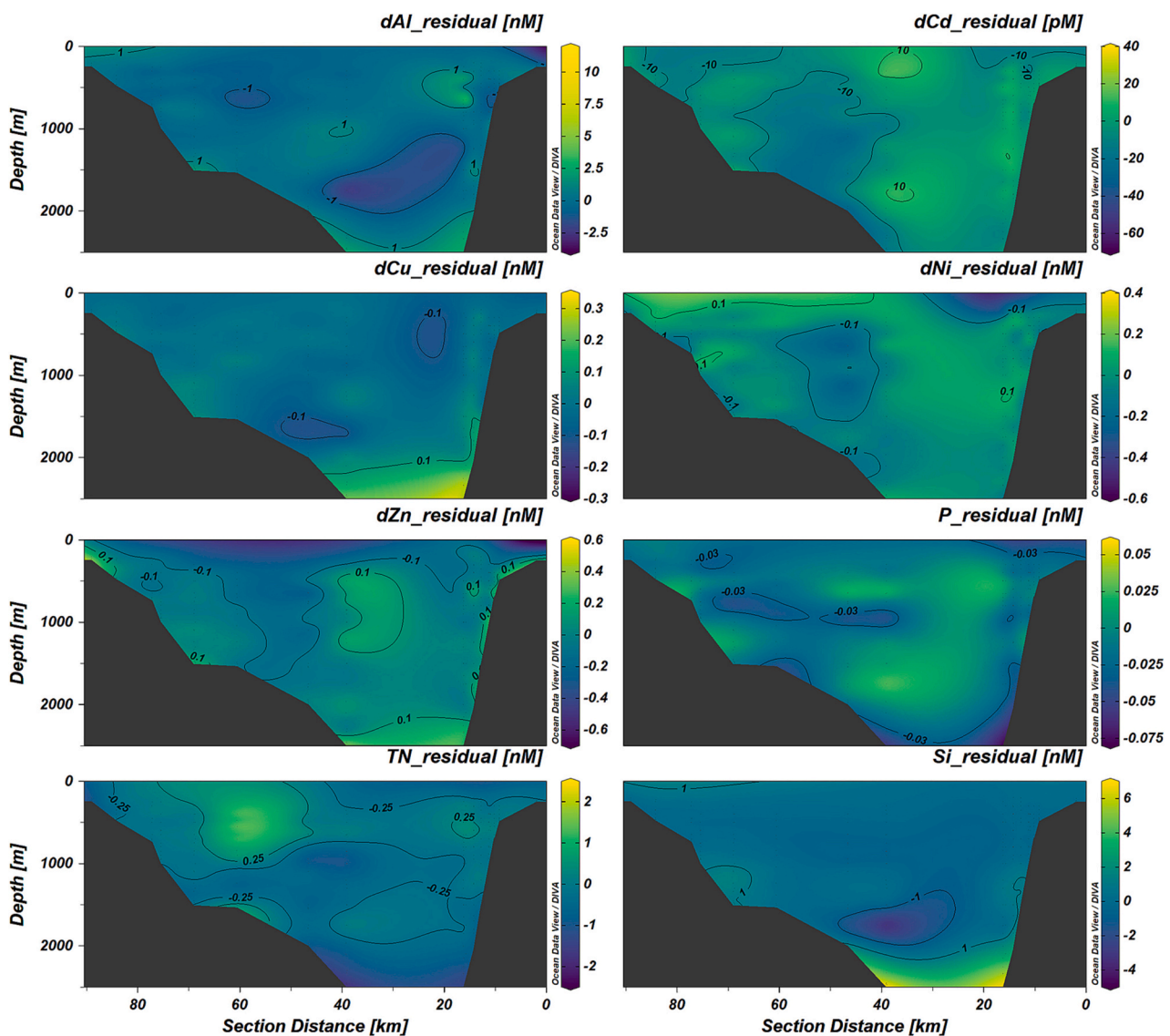
Fig. 6. The residuals (measured – modeled) of dTMs and nutrients along the slope transect.

to the continuous regeneration of dCd from sinking organic particles during water transport. In contrast, endmember dAl concentrations in MOW and NEADW are lower than the corresponding dAl levels at their formation region. This phenomenon is ascribed to scavenging removal of dAl during the transport of water masses. Because the OMP analysis refers to the local water masses rather than water masses in their

formation regions, our estimations on the apparent endmember concentrations of water masses are robust to show their relative chemical compositions.

The correlations between reconstructed dTMs and nutrients corresponded to the observed results, and no kinks were observed for the correlations between dCd, dNi, dZn, and P, while dCu:P and dAl:P ratios changed sharply at a density of 27.62 kg m^{-3} (depth ~ 1000 m) (Fig. 7). The dTM:AOU (except for dAl:AOU) and nutrient:AOU ratios changed abruptly at depths of ~1000 m and ~ 2000 m across all seasons (Fig. S2), coinciding with the variations in water mass fractions from MOW+SAIW+ENACW at 100–1000 m to MOW+NEADW+LSW at > ~ 1000 m. Therefore, the AOU variations at depth mostly reflect physical processes (e.g., water mass mixing) rather than local biological processes. All these observations indicate that subsurface dTMs and nutrients and their ratios on the NE Atlantic continental margin are mainly

controlled by water mass mixing driven by ocean circulation with local remineralization making a minor contribution.

3.4. The impact of MOW on the dTM distributions in the NE Atlantic Ocean

The dTM:nutrient and dTM:AOU kinks at ~1000 m and ~ 2000 m are closely related to the maximum and diminished occurrence of MOW (Fig. 4, Fig. S2), ascribed to the distinctive dTM and nutrient stoichiometry of MOW relative to other water masses (Table 2). For instance, MOW shows much higher dAl:P but lower dCu:P ratios than LSW and NEADW, thus creating kinks of dCu:P and dAl:P ratios at the maximum occurrence of MOW. Therefore, MOW provides an important imprint on the dTM distributions on the NE Atlantic continental slope.

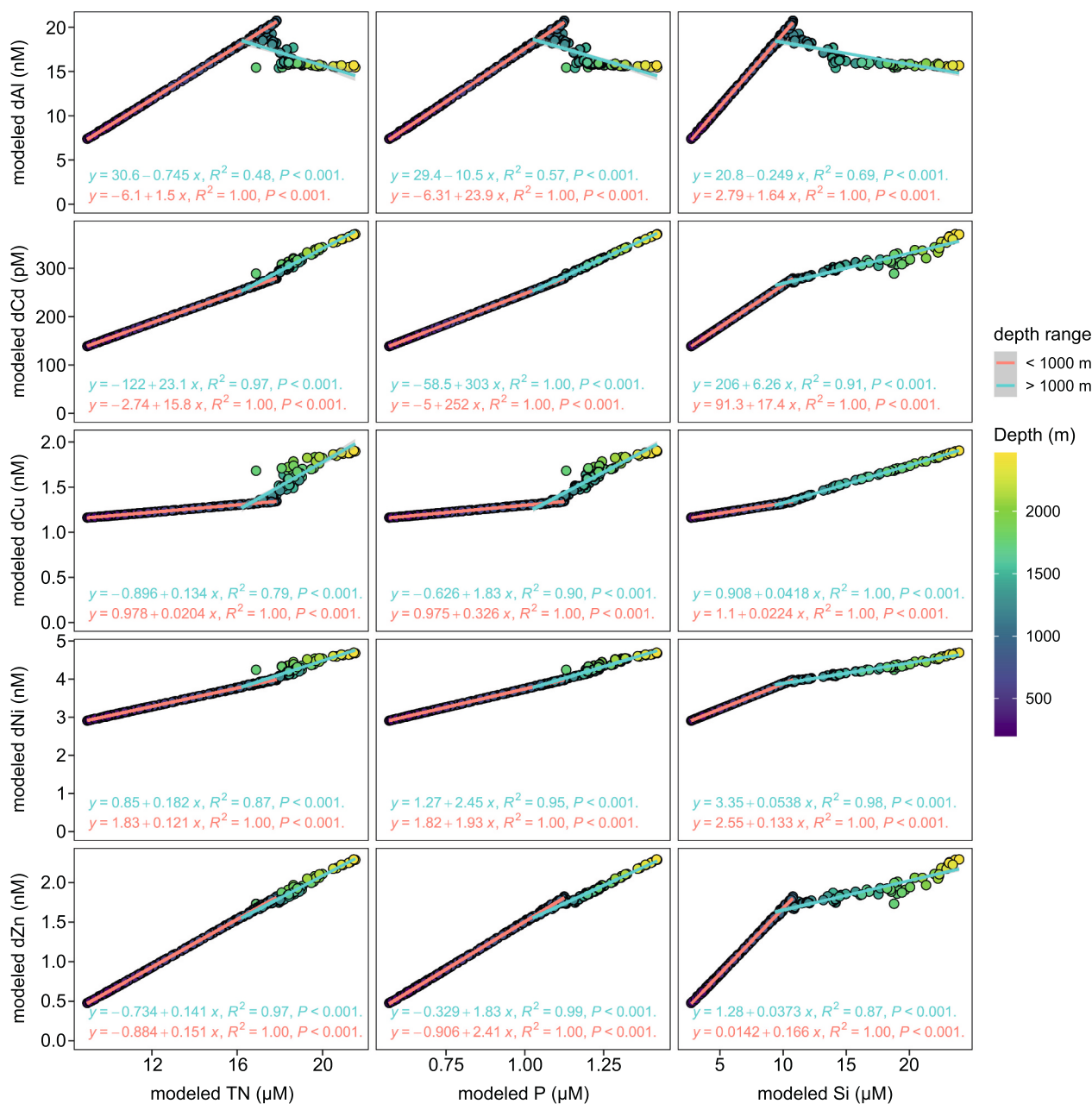The MOW is formed in the Mediterranean Sea and spreads across the

Fig. 7. Correlations between reconstructed dissolved trace metal (dTM: dAl, dCd, dCu, dNi, dZn) and nutrient (nitrate+nitrite [TN], phosphate [P], and silicic acid [Si]) concentrations on the Northeast Atlantic continental slope. Linear regression models were applied to depths <1000 m (potential density < 27.62 kg m^{-3}) and depths >1000 m (potential density > 27.62 kg m^{-3}), respectively.

NE Atlantic Ocean at ~500–1500 m towards the Bay of Biscay and further along the shelf break of the Celtic Sea (van Aken, 2000b; Price et al., 1993). The occurrence of MOW in the NE Atlantic Ocean can be observed in elevated dAl concentrations and salinity (Measures et al., 2015; Middag et al., 2022; Rolison et al., 2015) at depths of 900–1400 m. The significant correlations between dTMs and salinity (Fig. S10) demonstrate that dTMs in the MOW core were predominantly controlled by the conservative isopycnal mixing between MOW and lower salinity water masses (e.g., SAIW with similar density range to MOW; Johnson and Gruber, 2007) during ocean circulation, rather than removal by scavenging. Specifically, the dAl, dZn, and dNi concentrations of the MOW core decreased with decreasing salinity, suggesting the saline MOW is a net source to deliver Mediterranean-sourced Al, Zn, and Ni to the NE Atlantic Ocean (Middag et al., 2022). This finding is similar to the long-distance transport of anthropogenic Pb by MOW to the NE Atlantic continental margin (Rusiecka et al., 2018).

4. Conclusions

Our findings illustrate that the seasonal variations in surface dTMs and nutrient concentrations were associated with biological processes on the continental margin of the NE Atlantic Ocean. Surface dTM concentrations on the shelf were also influenced by a low-salinity end-member, likely fluvial discharge from the British Isles. Major temperate shelf seas like the Baltic Sea, Yellow Sea, Patagonian, Congo and Amazon shelf sea regions, are also recharged by large rivers which deliver abundant dissolved and particulate TMs (Gledhill et al., 2022; Vieira et al., 2020; Zhang, 1995). Global continental margins are usually characterized by the occurrence of fine sediments. However, our study suggested that benthic sedimentary inputs from local fine sediments played a minor role in the distribution of nutrient-type TMs in the NE Atlantic continental margin. Therefore, our results indicated that temperate shelf seas are influenced by local biological processes and external sources, where riverine inputs play an important role in delivering terrestrial dTMs to the open ocean. The dTM concentrations and metal:P ratios at depth in the slope region can be explained by water mass mixing without an important role for local remineralization processes. This underpins the importance of ocean circulation on the dTM distributions in global temperate shelf seas, where water masses with different origins converge along continental slopes. Specifically, the long-distance transport of MOW delivers Mediterranean-sourced dTMs (e.g., dAl, dZn, and Ni) into the NE Atlantic Ocean and drives dAl:P and dCu:P kinks at a potential density of ~27.62 kg m^{-3} (depth ~ 1000 m) along the NE Atlantic continental slope. Future climate change driven changes in water mass characteristics in the subpolar gyre, may have consequences for nutrient stoichiometry and hence the biological carbon cycles in the NE Atlantic Ocean.

Open research

Data are held at the British Oceanographic Data Centre (http://www.bodc.ac.uk/). The data in this study can be achieved by searching "Samples data" filtered by Cruise to "RRS Discovery DY018", "RRS Discovery DY029", and "RRS Discovery DY033".

Declaration of Competing Interest

None.

Data availability

Data are held at the British Oceanographic Data Centre (http://www.bodc.ac.uk/)

Appendix A. Supplementary data

Supplementary data to this article can be found online at https://doi.org/10.1016/j.marchem.2023.104246.

References

Achterberg, E.P., Colombo, C., van den Berg, C.M.G., 1999. The distribution of dissolved Cu, Zn, Ni, Co and Cr in English coastal surface waters. Cont. Shelf Res. 19, 537–558. https://doi.org/10.1016/S0278-4343(98)00093-4.

Achterberg, E.P., Steigenberger, S., Klar, J.K., Browning, T.J., Marsay, C.M., Painter, S.C., Vieira, L.H., Baker, A.R., Hamilton, D.S., Tanhua, T., Moore, C.M., 2021. Trace element biogeochemistry in the high-latitude North Atlantic Ocean: seasonal variations and volcanic inputs. Glob. Biogeochem. Cycles 35, e2020GB006674. https://doi.org/10.1029/2020GB006674.

Annett, A.L., Henley, S.F., Van Beek, P., Souhaut, M., Ganeshram, R., Venables, H.J., Meredith, M., Geibert, W., 2013. Use of radium isotopes to estimate mixing rates and trace sediment inputs to surface waters in northern Marguerite Bay, Antarctic Peninsula. Antarct. Sci. 25, 445–456. https://doi.org/10.1017/S0954102012000892.

Aphalo, P.J., 2022. ggpmisc: Miscellaneous Extensions to "ggplot2.".

Baars, O., Abouchami, W., Galer, S.J.G., Boye, M., Croot, P.L., 2014. Dissolved cadmium in the Southern Ocean: distribution, speciation, and relation to phosphate. Limnol. Oceanogr. 59, 385–399. https://doi.org/10.4319/lo.2014.59.2.0385.

Becker, S., Aoyama, M., Woodward, E.M.S., Bakker, K., Coverly, S., Mahaffey, C., Tanhua, T., 2020. GO-SHIP repeat hydrography nutrient manual: the precise and accurate determination of dissolved inorganic nutrients in seawater, using continuous flow analysis methods. Front. Mar. Sci. 7, 581790.

Birchill, A.J., 2017. The Seasonal Cycling and Physico-Chemical Speciation of iron on the Celtic and Hebridean Shelf Seas (Thesis).. University of Plymouth.

Birchill, A.J., Milne, A., Woodward, E.M.S., Harris, C., Annett, A., Rusiecka, D., Achterberg, E.P., Gledhill, M., Ussher, S.J., Worsfold, P.J., Geibert, W., Lohan, M.C., 2017. Seasonal iron depletion in temperate shelf seas. Geophys. Res. Lett. 44, 8987–8996. https://doi.org/10.1002/2017GL073881.

Boyd, P.W., Ellwood, M.J., Tagliabue, A., Twining, B.S., 2017. Biotic and abiotic retention, recycling and remineralization of metals in the ocean. Nat. Geosci. 10, 167–173. https://doi.org/10.1038/ngeo2876.

Boyle, E.A., 1988. Cadmium: chemical tracer of Deepwater paleoceanography. Paleoceanography 3, 471–489.

Boyle, E.A., Sclater, F., Edmond, J.M., 1976. On the marine geochemistry of cadmium. Nature 263, 42–44. https://doi.org/10.1038/263042a0.

Bruland, K.W., 1992. Complexation of cadmium by natural organic ligands in the central North Pacific. Limnol. Oceanogr. 37, 1008–1017. https://doi.org/10.4319/lo.1992.37.5.1008.

Bruland, K.W., Middag, R., Lohan, M.C., 2014. Controls of trace metals in seawater. In: Treatise on Geochemistry. Elsevier, pp. 19–51. https://doi.org/10.1016/B978-0-08-095975-7.00602-1.

Chen, X.-G., Rusiecka, D., Gledhill, M., Milne, A., Annett, A.L., Beck, A.J., Birchill, A.J., Lohan, M.C., Ussher, S., Achterberg, E.P., 2023. Physical and biogeochemical controls on seasonal iron, manganese, and cobalt distributions in Northeast Atlantic shelf seas. Geochim. Cosmochim. Acta 348, 278–295. https://doi.org/10.1016/j.gca.2023.03.023.

Cotté-Krief, M.-H., Thomas, A.J., Martin, J.-M., 2002. Trace metal (cd, cu, Ni and Pb) cycling in the upper water column near the shelf edge of the European continental margin (Celtic Sea). Mar. Chem. 79, 1–26. https://doi.org/10.1016/S0304-4203(02)00013-0.

Cullen, J.T., 2006. On the nonlinear relationship between dissolved cadmium and phosphate in the modern global ocean: could chronic iron limitation of phytoplankton growth cause the kink? Limnol. Oceanogr. 51, 1369–1380. https://doi.org/10.4319/lo.2006.51.3.1369.

Cutter, G., Casciotti, K., Croot, P., Geibert, W., Heimbürger, L.-E., Lohan, M., Planquette, H., van de Flierdt, T., 2017. Sampling and Sample-handling Protocols for

GEOTRACES Cruises. Version 3, August 2017. GEOTRACES Stand. Intercalibration Comm.

de Baar, H.J.W., Saager, P.M., Nolting, R.F., van der Meer, J., 1994. Cadmium versus phosphate in the world ocean. Mar. Chem. 46, 261–281. https://doi.org/10.1016/0304-4203(94)90082-5.

Frew, R.D., Hunter, K.A., 1992. Influence of Southern Ocean waters on the cadmium–phosphate properties of the global ocean. Nature 360, 144–146. https://doi.org/10.1038/360144a0.

García-Ibáñez, M.I., Pardo, P.C., Carracedo, L.I., Mercier, H., Lherminier, P., Ríos, A.F., Pérez, F.F., 2015. Structure, transports and transformations of the water masses in the Atlantic subpolar gyre. Prog. Oceanogr. 135, 18–36. https://doi.org/10.1016/j.pocean.2015.03.009.

García-Ibáñez, M.I., Pérez, F.F., Lherminier, P., Zunino, P., Mercier, H., Tréguer, P., 2018. Water mass distributions and transports for the 2014 GEOVIDE cruise in the North Atlantic. Biogeosciences 15, 2075–2090. https://doi.org/10.5194/bg-15-2075-2018.

Garcia-Solsona, E., Garcia-Orellana, J., Masqué, P., Dulaiova, H., 2008. Uncertainties associated with 223Ra and 224Ra measurements in water via a delayed coincidence counter (RaDeCC). Mar. Chem. 109, 198–219. https://doi.org/10.1016/j.marchem.2007.11.006.

GEOTRACES Intermediate Data Product Group, 2021. The GEOTRACES intermediate data product 2021 (IDP2021). NERC EDS British Oceanography Data Centre NOC. https://doi.org/10.5285/cf2d9ba9-d51d-3b7c-e053-8486abc0f5fd.

Gledhill, M., Hollister, A., Seidel, M., Zhu, K., Achterberg, E.P., Dittmar, T., Koschinsky, A., 2022. Trace metal stoichiometry of dissolved organic matter in the Amazon plume. Sci. Adv. 8, eabm2249. https://doi.org/10.1126/sciadv.abm2249.

Han, Q., Moore, J.K., Zender, C., Measures, C., Hydes, D., 2008. Constraining oceanic dust deposition using surface ocean dissolved Al. Glob. Biogeochem. Cycles 22, GB2003.

Ho, T.-Y., Quigg, A., Finkel, Z.V., Milligan, A.J., Wyman, K., Falkowski, P.G., Morel, F.M. M., 2003. The elemental composition of some marine Phytoplankton1. J. Phycol. 39, 1145–1159. https://doi.org/10.1111/j.0022-3646.2003.03-090.x.

Horner, T.J., Lee, R.B.Y., Henderson, G.M., Rickaby, R.E.M., 2013. Nonspecific uptake and homeostasis drive the oceanic cadmium cycle. Proc. Natl. Acad. Sci. 110, 2500–2505. https://doi.org/10.1073/pnas.1213857110.

Hu, X., Shi, X., Su, R., Jin, Y., Ren, S., Li, X., 2022. Spatiotemporal patterns and influencing factors of dissolved heavy metals off the Yangtze River Estuary, East China Sea. Mar. Pollut. Bull. 182, 113975 https://doi.org/10.1016/j.marpolbul.2022.113975.

Hydes, D.J., Liss, P.S., 1976. Fluorimetric method for the determination of low concentrations of dissolved aluminium in natural waters. Analyst 101, 922–931. https://doi.org/10.1039/an9760100922.

Janssen, D.J., Sieber, M., Ellwood, M.J., Conway, T.M., Barrett, P.M., Chen, X., de Souza, G.F., Hassler, C.S., Jaccard, S.L., 2020. Trace metal and nutrient dynamics across broad biogeochemical gradients in the Indian and Pacific sectors of the Southern Ocean. Mar. Chem. 221, 103773 https://doi.org/10.1016/j.marchem.2020.103773.

Johnson, G.C., Gruber, N., 2007. Decadal water mass variations along 20°W in the northeastern Atlantic Ocean. Prog. Oceanogr. 73, 277–295. https://doi.org/10.1016/j.pocean.2006.03.022.

Johnson, M.S., Meskhidze, N., Solmon, F., Gassó, S., Chuang, P.Y., Gaiero, D.M., Yantosca, R.M., Wu, S., Wang, Y., Carouge, C., 2010. Modeling dust and soluble iron deposition to the South Atlantic Ocean. J. Geophys. Res.-Atmos. 115 https://doi.org/10.1029/2009JD013311.

Kremling, K., Hydes, D., 1988. Summer distribution of dissolved Al, Cd, Co, Cu, Mn and Ni in surface waters around the British Isles. Cont. Shelf Res. 8, 89–105. https://doi.org/10.1016/0278-4343(88)90026-X.

Kremling, K., Pohl, C., 1989. Studies on the spatial and seasonal variability of dissolved cadmium, copper and nickel in Northeast Atlantic surface waters. Mar. Chem. 27, 43–60. https://doi.org/10.1016/0304-4203(89)90027-3.

La Fontaine, S., Quinn, J.M., Nakamoto, S.S., Page, M.D., Göhre, V., Moseley, J.L., Kropat, J., Merchant, S., 2002. Copper-dependent iron assimilation pathway in the model photosynthetic eukaryote Chlamydomonas reinhardtii. Eukaryot. Cell 1, 736–757.

Liu, M., Tanhua, T., 2021. Water masses in the Atlantic Ocean: characteristics and distributions. Ocean Sci. 17, 463–486. https://doi.org/10.5194/os-17-463-2021.

Lohan, M.C., Tagliabue, A., 2018. Oceanic micronutrients: trace metals that are essential for marine life. Elements 14, 385–390. https://doi.org/10.2138/gselements.14.6.385.

Mahaffey, C., Reynolds, S., Davis, C.E., Lohan, M.C., 2014. Alkaline phosphatase activity in the subtropical ocean: insights from nutrient, dust and trace metal addition experiments. Front. Mar. Sci. 1, 73.

Measures, C., Edmond, J.M., 1988. Aluminium as a tracer of the deep outflow from the Mediterranean. J. Geophys. Res. Oceans 93, 591–595. https://doi.org/10.1029/JC093iC01p00591.

Measures, C., Hatta, M., Fitzsimmons, J., Morton, P., 2015. Dissolved Al in the zonal N Atlantic section of the US GEOTRACES 2010/2011 cruises and the importance of hydrothermal inputs. Deep-Sea Res. II Top. Stud. Oceanogr. 116, 176–186. https://doi.org/10.1016/j.dsr2.2014.07.006.

Menzel Barraqueta, J.-L., Schlosser, C., Planquette, H., Gourain, A., Cheize, M., Boutorh, J., Shelley, R., Contreira Pereira, L., Gledhill, M., Hopwood, M.J., Lacan, F., Lherminier, P., Sarthou, G., Achterberg, E.P., 2018. Aluminium in the North Atlantic Ocean and the Labrador Sea (GEOTRACES GA01 section): roles of continental inputs and biogenic particle removal. Biogeosciences 15, 5271–5286. https://doi.org/10.5194/bg-15-5271-2018.

Menzel Barraqueta, J.-L., Klar, J.K., Gledhill, M., Schlosser, C., Shelley, R., Planquette, H. F., Wenzel, B., Sarthou, G., Achterberg, E.P., 2019. Atmospheric deposition fluxes over the Atlantic Ocean: a GEOTRACES case study. Biogeosciences 16, 1525–1542. https://doi.org/10.5194/bg-16-1525-2019.

Middag, R., van Heuven, S.M.A.C., Bruland, K.W., de Baar, H.J.W., 2018. The relationship between cadmium and phosphate in the Atlantic Ocean unravelled. Earth Planet. Sci. Lett. 492, 79–88. https://doi.org/10.1016/j.epsl.2018.03.046.

Middag, R., Rolison, J.M., George, E., Gerringa, L.J.A., Rijkenberg, M.J.A., Stirling, C.H., 2022. Basin scale distributions of dissolved manganese, nickel, zinc and cadmium in the Mediterranean Sea. Mar. Chem. 238, 104063 https://doi.org/10.1016/j.marchem.2021.104063.

Moore, W.S., 2008. Fifteen years experience in measuring 224Ra and 223Ra by delayed-coincidence counting. Mar. Chem. 109, 188–197.

Moore, W.S., Arnold, R., 1996. Measurement of 223Ra and 224Ra in coastal waters using a delayed coincidence counter. J. Geophys. Res. Oceans 101, 1321–1329. https://doi.org/10.1029/95JC03139.

Moore, C.M., Mills, M.M., Arrigo, K.R., Berman-Frank, I., Bopp, L., Boyd, P.W., Galbraith, E.D., Geider, R.J., Guieu, C., Jaccard, S.L., Jickells, T.D., La Roche, J., Lenton, T.M., Mahowald, N.M., Marañón, E., Marinov, I., Moore, J.K., Nakatsuka, T., Oschlies, A., Saito, M.A., Thingstad, T.F., Tsuda, A., Ulloa, O., 2013. Processes and patterns of oceanic nutrient limitation. Nat. Geosci. 6, 701–710. https://doi.org/10.1038/ngeo1765.

Mora, A., Alfonso, J.A., Sánchez, L., Calzadilla, M., Silva, S., LaBrecque, J.J., Azócar, J. A., 2009. Temporal variability of selected dissolved elements in the lower Orinoco River, Venezuela. Hydrol. Process. 23, 476–485. https://doi.org/10.1002/hyp.7159.

Morel, F.M.M., Price, N.M., 2003. The biogeochemical cycles of trace metals in the oceans. Science 300, 944–947.

Morel, F.M.M., Reinfelder, J.R., Roberts, S.B., Chamberlain, C.P., Lee, J.G., Yee, D., 1994. Zinc and carbon co-limitation of marine phytoplankton. Nature 369, 740–742. https://doi.org/10.1038/369740a0.

Muller-Karger, F.E., Varela, R., Thunell, R., Luerssen, R., Hu, C., Walsh, J.J., 2005. The importance of continental margins in the global carbon cycle. Geophys. Res. Lett. 32, L01602.

Olsen, A., Lange, N., Key, R.M., Tanhua, T., Álvarez, M., Becker, S., Bittig, H.C., Carter, B. R., Cotrim da Cunha, L., Feely, R.A., van Heuven, S., Hoppema, M., Ishii, M., Jeansson, E., Jones, S.D., Jutterström, S., Karlsen, M.K., Kozyr, A., Lauvset, S.K., Lo Monaco, C., Murata, A., Pérez, F.F., Pfeil, B., Schirnick, C., Steinfeldt, R., Suzuki, T., Telszewski, M., Tilbrook, B., Velo, A., Wanninkhof, R., 2019. GLODAPv2.2019 – an update of GLODAPv2. Earth Syst. Sci. Data 11, 1437–1461. https://doi.org/10.5194/essd-11-1437-2019.

Price, N.M., Morel, F.M.M., 1990. Cadmium and cobalt substitution for zinc in a marine diatom. Nature 344, 658–660.

Price, J.F., Baringer, M.O., Lueck, R.G., Johnson, G.C., Ambar, I., Parrilla, G., Cantos, A., Kennelly, M.A., Sanford, T.B., 1993. Mediterranean outflow mixing and dynamics. Science 259, 1277–1282. https://doi.org/10.1126/science.259.5099.1277.

Rapp, I., Schlosser, C., Rusiecka, D., Gledhill, M., Achterberg, E.P., 2017. Automated preconcentration of Fe, Zn, Cu, Ni, Cd, Pb, Co, and Mn in seawater with analysis using high-resolution sector field inductively-coupled plasma mass spectrometry. Anal. Chim. Acta 976, 1–13. https://doi.org/10.1016/j.aca.2017.05.008.

Reinthaler, T., Álvarez Salgado, X.A., Álvarez, M., van Aken, H.M., Herndl, G.J., 2013. Impact of water mass mixing on the biogeochemistry and microbiology of the Northeast Atlantic deep water. Glob. Biogeochem. Cycles 27, 1151–1162. https://doi.org/10.1002/2013GB004634.

Revelle, W.R., 2017. psych: Procedures for Personality and Psychological Research.

Rolison, J.M., Middag, R., Stirling, C.H., Rijkenberg, M.J.A., de Baar, H.J.W., 2015. Zonal distribution of dissolved aluminium in the Mediterranean Sea. Mar. Chem. 177, 87–100. https://doi.org/10.1016/j.marchem.2015.05.001.

Roshan, S., DeVries, T., 2021. Global contrasts between oceanic cycling of cadmium and phosphate. Glob. Biogeochem. Cycles 35, e2021GB006952. https://doi.org/10.1029/2021GB006952.

Roshan, S., Wu, J., 2015. Cadmium regeneration within the North Atlantic. Glob. Biogeochem. Cycles 29, 2082–2094. https://doi.org/10.1002/2015GB005215.

Rusiecka, D., Gledhill, M., Milne, A., Achterberg, E.P., Annett, A.L., Atkinson, S., Birchill, A.J., Karstensen, J., Lohan, M., Mariez, C., Middag, R., Rolison, J.M., Tanhua, T., Ussher, S., Connelly, D., 2018. Anthropogenic signatures of lead in the Northeast Atlantic. Geophys. Res. Lett. 45, 2734–2743. https://doi.org/10.1002/2017GL076825.

Saager, P.M., de Baar, H.J.W., de Jong, J.T.M., Nolting, R.F., Schijf, J., 1997. Hydrography and local sources of dissolved trace metals Mn, Ni, cu, and cd in the Northeast Atlantic Ocean. Mar. Chem. 57, 195–216. https://doi.org/10.1016/S0304-4203(97)00038-8.

Saito, M.A., Goepfert, T.J., Noble, A.E., Bertrand, E.M., Sedwick, P.N., DiTullio, G.R., 2010. A seasonal study of dissolved cobalt in the Ross Sea, Antarctica: micronutrient behavior, absence of scavenging, and relationships with Zn, cd, and P. Biogeosciences 7, 4059–4082. https://doi.org/10.5194/bg-7-4059-2010.

Schlitzer, R., 2021. Ocean Data View. odv.awi.de.

Simpson, J.H., Sharples, J., 2012. Introduction to the Physical and Biological Oceanography of Shelf Seas. Cambridge University Press.

Sun, Y., Torgersen, T., 1998. The effects of water content and Mn-fiber surface conditions on measurement by emanation. Mar. Chem. 62, 299–306. https://doi.org/10.1016/S0304-4203(98)00019-X.

Sunda, W.G., Huntsman, S.A., 2000. Effect of Zn, Mn, and Fe on cd accumulation in phytoplankton: implications for oceanic cd cycling. Limnol. Oceanogr. 45, 1501–1516.

Thomas, H., Bozec, Y., Elkalay, K., de Baar, H.J.W., 2004. Enhanced Open Ocean storage of CO2 from Shelf Sea pumping. Science 304, 1005–1008. https://doi.org/10.1126/science.1095491.

Twining, B.S., Baines, S.B., 2013. The trace metal composition of marine phytoplankton. Annu. Rev. Mar. Sci. 5, 191–215. https://doi.org/10.1146/annurev-marine-121211-172322.

van Aken, H.M., 2000a. The hydrography of the mid-latitude Northeast Atlantic Ocean: I: the deep water masses. Deep-Sea Res. I Oceanogr. Res. Pap. 47, 757–788. https://doi.org/10.1016/S0967-0637(99)00092-8.

van Aken, H.M., 2000b. The hydrography of the mid-latitude Northeast Atlantic Ocean: II: the intermediate water masses. Deep-Sea Res. I Oceanogr. Res. Pap. 47, 789–824. https://doi.org/10.1016/S0967-0637(99)00112-0.

Vieira, L.H., Krisch, S., Hopwood, M.J., Beck, A.J., Scholten, J., Liebetrau, V., Achterberg, E.P., 2020. Unprecedented Fe delivery from the Congo River margin to the South Atlantic gyre. Nat. Commun. 11, 556. https://doi.org/10.1038/s41467-019-14255-2.

Waeles, M., Riso, R.D., Le Corre, P., 2005. Seasonal variations of dissolved and particulate copper species in estuarine waters. Estuar. Coast. Shelf Sci. 62, 313–323. https://doi.org/10.1016/j.ecss.2004.09.019.

Wickham, H., Averick, M., Bryan, J., Chang, W., McGowan, L.D., François, R., Grolemund, G., Hayes, A., Henry, L., Hester, J., Kuhn, M., Pedersen, T.L., Miller, E., Bache, S.M., Müller, K., Ooms, J., Robinson, D., Seidel, D.P., Spinu, V., Takahashi, K.,

Vaughan, D., Wilke, C., Woo, K., Yutani, H., 2019. Welcome to the Tidyverse. J. Open Source Softw. 4, 1686. https://doi.org/10.21105/joss.01686.

Woodward, E.M.S., Rees, A.P., 2001. Nutrient distributions in an anticyclonic eddy in the Northeast Atlantic Ocean, with reference to nanomolar ammonium concentrations. Deep-Sea Res. II Top. Stud. Oceanogr. 48, 775–793. https://doi.org/10.1016/S0967-0645(00)00097-7.

Wu, J., Roshan, S., 2015. Cadmium in the North Atlantic: implication for global cadmium–phosphorus relationship. Deep-Sea Res. II Top. Stud. Oceanogr. 116, 226–239. https://doi.org/10.1016/j.dsr2.2014.11.007.

Wyatt, N.J., Milne, A., Woodward, E.M.S., Rees, A.P., Browning, T.J., Bouman, H.A., Worsfold, P.J., Lohan, M.C., 2014. Biogeochemical cycling of dissolved zinc along the GEOTRACES South Atlantic transect GA10 at 40°S. Glob. Biogeochem. Cycles 28, 44–56. https://doi.org/10.1002/2013GB004637.

Xie, R.C., Galer, S.J.G., Abouchami, W., Rijkenberg, M.J.A., De Jong, J., de Baar, H.J.W., Andreae, M.O., 2015. The cadmium–phosphate relationship in the western South Atlantic — the importance of mode and intermediate waters on the global systematics. Mar. Chem. 177, 110–123. https://doi.org/10.1016/j.marchem.2015.06.011.

Zhang, J., 1995. Geochemistry of trace metals from Chinese River/estuary systems: an overview. Estuar. Coast. Shelf Sci. 41, 631–658. https://doi.org/10.1006/ecss.1995.0082.